Modeling And Simulation of A High Pressure Roller Crusher for Silicon Carbide Production

Sylvester Sedem Djokoto
Department of Engineering, Faculty of Engineering and Science, University of Agder, N-4898 Grimstad, Norway
e-mail: ssdjok03@student.uia.no

Hamid Reza Karimi
Department of Engineering, Faculty of Engineering and Science, University of Agder, N-4898 Grimstad, Norway
e-mail: hamid.r.karimi@uia.no

Abstract— **This paper describes the modeling and simulation of High Pressure Roller Crusher (HPRC) for the production of silicon carbide grains. The study is to make a model for simulation of a High Pressure Roller Crusher. A High Pressure Roller Crusher (HPRC) is an important part in the production of silicon carbide, where the grains are crushed into powder form and then sieved into specified sizes based on its usage. This paper will present a model based on Johanson's theory for roller compactors, considering all the delays. The non-linearity or delays were handled using Matlab software. Conclusions are given at end of the paper.**

Keywords: High Pressure Roller Crusher (HPRC), Silicon Carbide, Padè approximation

I. INTRODUCTION

The discovery of silicon carbide dated back to about 100 years ago, when a struggling scientist, once employed by Thomas Edison, dreamed of becoming wealthy. What is a better way to riches, he reasoned, than by making artificial diamonds?

This young scientist, Dr. Edward Goodrich Acheson, had invented silicon carbide (SiC), the first man-made abrasive and substance hard enough to cut glass.

Saint Gobain Ceremics Norway is one the leading producers of Silicon Carbide. The milling process of silicon carbide happens at different stages. The Arendal branch of this company produces Silicon Carbide grain into different sizes that is turned into slurry to aid the cutting of solar cells.

The modeling and simulation of the roller compactor will be an integral part of the process such that suitable controllers could be designed in the future. This paper considered a two input and two output model design based on Johanson's theory for roller compactors. Due to non linearity a Padè approximation approach was used to linearize the system. The modeling was done using Matlab tools and Simulink to verify the model.

II. MILLING PROCESS

A. Silicon Carbide Production and its properties

Acheson's discovery of Silicon Carbide became Carborundum, the trademark for silicon carbide and the name given to the company he started. No other company in the world that has more expertise with silicon carbide than Saint-Gobain. They invented it, developed numerous variations of it and make more of it for high-performance components than anyone else in the world. Saint Gobain has companies in Arendal and Lillesand in Norway for the production of Silicon Carbide (SiC)

Today Saint-Gobain has earned a reputation for providing advanced, high-tech ceramic components to worldwide markets. These markets span multiple industries, requiring materials that are resistant to extreme temperature, thermal shock, abrasion and corrosion.

Silicon Carbide (SiC) is a material that is very useful for different purposes. It has properties such as:

- High hardness (only diamond is harder), compressive strength and light weight. Hardness (Knoop): 2800 kg/mm2 at room temperature
- It exhibits reduced micro porosity resulting in a higher Weibull modulus and increased flexural strength Flexural strength (4 pt.): 55,000 psi (380 MPa) Fracture toughness: 4.20 x 103 lb/in2 x in½ Modulus of elasticity (RT): 59 x 106 lb/in2 (410 GPa)
- Very good temperature resistance; the thermal conductivity of silicon carbide, combined with its low thermal expansion, produces excellent thermal-shock resistance far better than tungsten carbide, aluminum oxide and RB silicon nitride. These properties make it a promising candidate to replace ductile metals in high-temperature applications.
- It's wear resistant**;** the extreme hardness and density of silicon carbide make it ideal for applications where parts are subject to high abrasion and sliding wear. Specified wear rate (pin on disc): SiC vs. SiC 1 x 10-9 mm2/kg. Coefficient of friction (pin on disc): SiC vs. SiC 0.2.

- It resists corrosion, oxidation and erosion. The high density, low porosity and chemical inertness of silicon carbide permit it to function in environments of hot gases and liquids, in oxidizing and corrosive atmospheres, and in strong acids and bases, even at extremely high temperatures.
- It requires minimum machining. The surface finish of silicon carbide parts is excellent (about 64 micro inches). This surface quality, combined with tight dimensional control, yields parts that should require little or no additional machining or finish grinding, depending on application.

The properties above allow for a variety of applications such as:

- Cutting and grinding of hard materials, including silicon wafers for solar cells
- Diesel Particulate Filter (Automotive industries) (re crystallized SiC)
- Bushings in the aluminum electrolysis (electrical and electronic industries)
- Linings of furnaces (Process industry)
- Seal water pumps (sintered SiC) (Hydraulic, hydro chemical industries)
- Bullet- proof vests, armor vehicles

The milling process involves many parameters and this in turn affects the quality, weight percentage of product residue on the sieve with definite size. The output of this plant is the particle sizes of the SiC product based on the customer's request. A dynamic model is therefore necessary to develop a controller for the thickness of the flake that is coming out from the crusher.

B. Working Princinples of the High Pressure Roller Crusher

High Pressure Roller Crusher (HPRC) or High Pressure Grinding Rolls (HPGR) was introduced as a new grinding technology in 1984. Since then, they have been successfully installed in a large number of plants throughout the world, mainly for cement and limestone. More recently, HPGRs have also been applied in mineral processing plants, largely in iron ore and diamond treatment. In these industries, the application of HPGR ranges from coarse grinding, e.g. the grinding of 65mm (2.5") size excess pebbles in AG circulation loops, to final grinding of <100μm material to high Blaine values in the preparation of pellet feed [1].

High Pressure Grinding Rolls (HPGR) offers several benefits to the minerals industry, such as:

- Low energy consumption, 0.8-3.0kWh/t
- Ability to process moist ores, up to 10%
- Enhanced downstream recovery and grindability
- Improved grade of downstream products
- Low maintenance requirements
- Low space requirements
- Low vibration and noise
- High availability, >95%

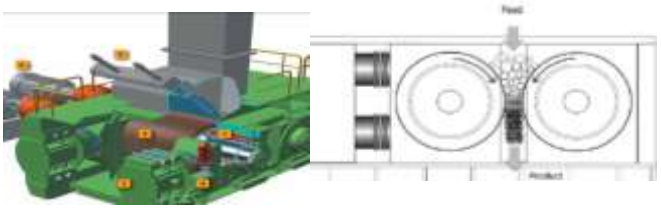

Figure 1.Cross-sectional representation of HPGR, including the hydraulic spring system

1. Press frame
2. Press rolls
3. Bearing system
4. Hydraulic pressing device
5. Feeding device
6. Drive

The feed to the crusher is usually dry. Moisture tends to clog the crusher and could result in the formation of hard crust. Rock particles or dry granulation are fed through chute designed to distribute the charge evenly along the width of the roll. About two-thirds of the roll-width is active. In any crusher, the particle sizes less than the distance between the rolls tend to pass through uncrushed. Particles that is larger than the opening is nipped and crushed. The maximum size of particle that is nipped without slippage depends on friction, distance between the rolls and roll size [2, 3].

The size of the product depends on the crusher set, the distance between the rolls. Due to single pass operation it is evident that no middlings or over-size is produced.

The normal speed of operation of commercial light duty rolls is 130-300 rpm compared to heavy duty rolls whose operating speeds are in the region of 80-100 rpm. Regulated slow rate of feeding spread over evenly across the width of the rolls is preferred when close circuit operation is adopted for finer product size.

The Morrell/Tondo/Shi model consists of three parts, namely a model for the prediction of product size distribution, a throughput model, and power consumption component. The throughput model component uses a standard plug flow model version that has been used extensively by the manufacturers and researchers. The power consumption is based on the throughput and the specific comminution energy (Ecs) input [4].

II DYNAMIC MODEL FOR ROLLER PROCESS

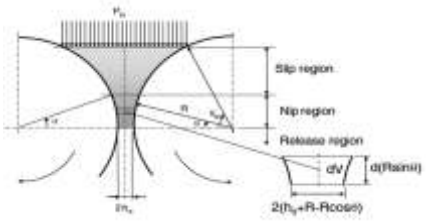

Figure 1 Johanson's Rolling Theory

The study will focus on the dynamic model of a roller compactor as described in Shuo-Huan Hsu & Gintaras V. Reklaitis 2010 using Johanson' approach. Johanson was the first to come out with a mathematical model for granulated materials. The roll press has been used widely in the still industry. Johanson provided a means to determine the press dimensions and roll forces necessary to apply the required pressure to a material with specific properties which were attained experimentally [5].

The crusher is assumed to have one fixed and one movable roll. The process parameters of the roller compactor are the speed of the roll (in rpm) and the roll pressure (in MPa). The output variables are the flake density (in g/cm3) and the gap width (in mm). Using Young's modulus and tensile strength a model can be derived [6]. It was shown by experiments [7] that the roll pressure and gap width have influence on the ribbon density at steady state, but not roll speed. On the other hand, the roll gap decreases when increasing the roll pressure and keeping other parameters constants [8]. The roll gap width is also influenced by the speeds of the feed screw and rolls. In Johanson's model the gap width is assumed to be constant which is impossible to predict the response of the gap width when the parameters are changed. [9] The material balance equation is introduced to model the characteristics of the gap width change [10].

In Johanson's theory three areas of the material behavior in the roller compaction: slip, nip and release region were considered as shown in the figure above.

The Slip region:

From Jenike and Shield effective yield function:

$$\frac{d\sigma}{d\theta} = -\frac{4\sigma\left(\frac{\pi}{2}-\theta-v\right)\tan\delta}{\left(1+\frac{h_0}{R}-\cos\theta\right)\left[\frac{1}{\tan(\beta-\mu)}-\frac{1}{\tan(\beta+\mu)}\right]} \quad (1)$$

Where:

$$\mu = \frac{\pi}{4}-\frac{\delta}{2}, v = \frac{1}{2}\left(\pi - \sin^{-1}\frac{\sin\emptyset}{\sin\delta} - \emptyset\right), \quad (2)$$

$$B = \frac{1}{2}\left(\frac{1}{2}+\emptyset+v\right)$$

δ is the effective angle of friction,
∅ is angle of surface friction,
h0 is half of the roll gap, and
R is the radius of the roll.
δ and ∅ are determined by the experiments.

In the nip region, an empirical model is used to describe the compression behavior of the material given by:

$$\sigma = C_1\rho^K \quad (3)$$

where:
σ is the material stress
ρ is the compact density
C_1 and K are constants

The nip angle is important boundary information for other models for rolling compaction of powders. It defines one of the limits for the region where most of the compaction is believed to take place. Therefore it is important to become familiar with the process and powder parameters influence on the behavior of this angle. Although it is very difficult to measure the nip angle, literature exists and states that the model provides a good estimate of the nip angle. The results are in agreement with experimental data especially for gravity fed roller presses [11].

The Nip region is given as:

$$\frac{\sigma(\theta)}{\sigma(\alpha)} = \left[\frac{\left(1+\frac{h_0}{R}-\cos\theta\right)\cos\alpha}{\left(1+\frac{h_0}{R}-\cos\theta\right)\cos\theta}\right]^K \quad (4)$$

Nip angle is given as:

$$\left(\frac{d\sigma}{d\theta}\right)_{slip} = \left(\frac{d\sigma}{d\theta}\right)_{nip} \quad (5)$$

At $\theta = \alpha$

Roll Force, F is giving as:

$$F = \frac{\sigma_{exit}\,R}{1+\sin\delta}\int_0^\alpha \left[\frac{\frac{h_0}{R}}{\left(1+\frac{h_0}{R}-\cos\theta\right)\cos\theta}\right]^K \cos\theta d\theta \quad (6)$$

where:
σexit=σ (θ = 0).
Ph is the hydraulic pressure applied on the roll and it is designed to resist this force [5]

$$F = \frac{A}{W}P_h \quad (7)$$

Rewriting equation (7)

$$P_h = \frac{A}{W}\frac{\sigma_{exit}\,R}{1+\sin\delta}\int_0^\alpha \left[\frac{\frac{h_0}{R}}{\left(1+\frac{h_0}{R}-\cos\theta\right)\cos\theta}\right]^K \cos\theta d\theta \quad (8)$$

where A is the compact area.

From Johanson' rolling theory the following were the limitations:

- No time dependency
  - Predict steady state behaviors
  - Not suitable for control purpose
- The effects of the roll speed and speed are not considered
- The physical and mechanical properties of the material do not change

An important parameter for the initial conditions to solve equation (1) is the feed pressure.

However, in most designs today, the feed flow is driven by one or two augers. The auger aims to stabilize the feed flow. Due to the poor flowability, the auger filling may fluctuate from one revolution to another [12]. The auger provides much higher pressure than the pressure caused by the gravity, and hence the gravity effect is negligible.

Therefore, Johanson's model can be used to predict the system with not only vertically mounted rolls, but also other

orientations. It is very difficult to predict the feed pressure provided by the auger [13].

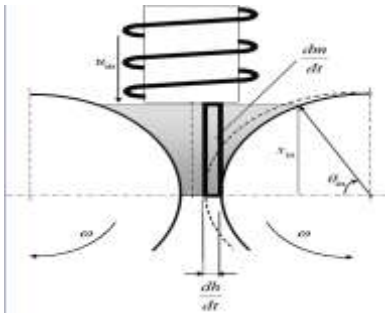

Figure 3 Johanson's mass balance model

Material Balance is given as:

$$\frac{dm}{dt} = \dot{m}_{in} - \dot{m}_{out} \tag{9}$$

$$= \rho_{in} u_{in} W(h_o + R - R\cos\theta_{in}) - \rho_{exit} R\omega W \tag{10}$$

$$\Delta m = \left[\int_0^{x_{in}} \rho dx\right] W \Delta h \tag{11}$$

$$\frac{d}{dt}\left(\frac{h_0}{R}\right) = \frac{\omega\left[\rho_{in}\cos\theta_{in}\left(\frac{u_{in}}{\omega R}\right)\left(\frac{h_0}{R}+1-\cos\theta_{in}\right)-\rho_{exit}\left(\frac{h_0}{R}\right)\right]}{\int_0^{\theta m}\rho(\theta)\cos\theta d\theta} \tag{12}$$

Equation (12) introduces the time dependency to the roller compaction model. The inlet–outlet speed ratio (uin/ωR) directly affects the roll gap change, and the density profile ρ(θ) needs to be solved for each time step.
In the nip region, ρ(θ) can be easily calculated using Eq. (9), but the density–stress relationship in the slip region is not clear. Since the stress is relatively small in the slip region and does not vary in a wide range, it is further assumed that the density in this region is a constant, i.e., the same as the inlet density. With this assumption, the denominator of the right hand side of
Eq. (12) can be solved analytically:

$$\int_0^{\theta_m} \rho(\theta)\cos\theta d\theta$$

$$= \rho_{exit}\left(\frac{h_0}{R}\right)\left\{\frac{2\left(1+\frac{h_0}{R}\right)}{\sqrt{\frac{h_0}{R}\left(2+\frac{h_0}{R}\right)}}\tan^{-1}\left[\sqrt{1+\frac{2R}{h_0}}\tan\frac{\alpha}{2}\right]-\alpha\right\}$$

$$+ \rho_{in}(\cos v - \sin\alpha$$

where:
θin=π/2−ν,
xin=Rsinθin,
ω is the angular velocity of the rolls, and
uin is the linear velocity of the feed, which is proportional to the rotational speed of the feed auger.

C. Model Representation

Hence, the transfer function matrix of the process G(s) is the following:

Modeling using state space transfer matrix

The transfer function in the Laplace domain is given as:

$$sx(s) = Ax(s) + Bu(s) \tag{13}$$

$$y(s) = Cx(s) + Du(s) \tag{14}$$

Eliminating $x(s)$ the using equation (13) and inserting the expression into equation (14) gives;

$$y(s) = [C(sI - A)^{-1}B + D]u(s) \tag{15}$$

The transfer function $H(s)$ from $u(s)$ to (s) :

$$H(s) = [C(sI - A)^{-1}B + D] \tag{16}$$

where

$$\frac{y}{u}(s) = H(s) \tag{17}$$

The figure shows system with two inputs and two outputs:

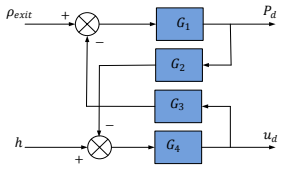

Figure.4 two input two output structure.

This will end with the transfer matrix;

$$\begin{bmatrix}\rho_{exist}\\ h\end{bmatrix} = \begin{bmatrix}\frac{G_1}{1-G_1G_2G_3G_4} & -\frac{G_1G_3G_4}{1-G_1G_2G_3G_4}\\ -\frac{G_1G_2G_4}{1-G_1G_2G_3G_4} & \frac{G_4}{1-G_1G_2G_3G_4}\end{bmatrix}\begin{bmatrix}P_d\\ u_d\end{bmatrix} \tag{18}$$

D. Time delays

Time delays are common phenomena in many industrial processes [14]. Suppose a multivariable delayed system is defined as $\widehat{G_1}(s)$, in which every component is described as $gij(s)e^{-sTij}$ for i = 1, 2,…., $p1$ and j= 1,2,…,m1. The structure of the delayed multivariable system is shown in Fig. 5. In order to obtain a rational transfer function, the time delay term can be approximated by a first order
Padè approximation model [15, 16] as,

$$e^{-sT} \approx \frac{2-sT}{2+sT} \quad (19)$$

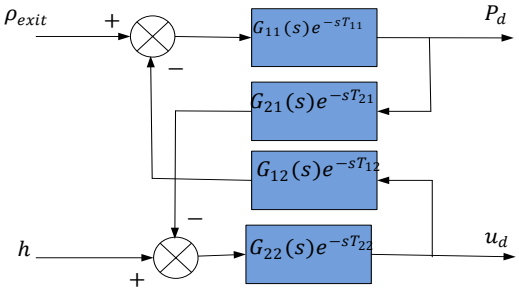

Figure 5. A delayed multivariable (2 x 2) system structure.

The state space representation with delay is given as;

$$y(s) = G(s)u(s)$$

where

$$\begin{bmatrix} G_{11}(s) & G_{12}(s) \\ G_{21}(s) & G_{22}(s) \end{bmatrix} = \begin{bmatrix} \frac{0.2615\,e^{-2.2676\,s}}{5.8313\,s+1} & \frac{-0.0475\,e^{-2.2854\,s}}{5.8396\,s+1} \\ \frac{-1.5163\,e^{-3.5197\,s}}{5.8694\,s+1} & \frac{1.6863\,e^{-2.1068\,s}}{5.8097\,s+1} \end{bmatrix}$$

$$y(s) = [\rho_{exist}(s)h(s)]^T,$$

$$u(s) = [P_d(s)u_d(s)]^T$$

III SIMULATION RESULTS

Padé approximations are used to approximate the delay terms. With the use of Simulink, the accurate model can be established as shown in Figure 6.When the Simulink model is established, the following statements can be used in the linearization process, and one can obtain the linear state space model. The exact simulation results are obtained, together with the linearized model, as shown in Figure. It can be seen that the simulation results of the linearized model are very accurate [17].

$$\dot{x} = \begin{bmatrix} -1.054 & -0.3026 & 0 & 0 & 0 & 0 & 0 & 0 \\ 0.5 & 0 & 0 & 0 & 0 & 0 & 0 & 0 \\ 0 & 0 & -0.7386 & -0.3872 & 0 & 0 & 0 & 0 \\ 0 & 0 & 0.25 & 0 & 0 & 0 & 0 & 0 \\ 0 & 0 & 0 & 0 & -0.8719 & -0.48 & 0 & 0 \\ 0 & 0 & 0 & 0 & 0.25 & 0 & 0 & 0 \\ 0 & 0 & 0 & 0 & 0 & 0 & -1.121 & -0.3268 \\ 0 & 0 & 0 & 0 & 0 & 0 & 0.5 & 0 \end{bmatrix} x$$

$$+ \begin{bmatrix} 0.25 & 0 \\ 0 & 0 \\ 1 & 0 \\ 0 & 0 \\ 0 & 0.125 \\ 0 & 0 \\ 0 & 1 \\ 0 & 0 \end{bmatrix} u$$

$$y = \begin{bmatrix} -0.1485 & 0.262 & 0 & 0 & 0.06507 & -0.1824 & 0 & 0 \\ 0 & 0 & 0.2583 & -0.5872 & 0 & 0 & -0.2903 & 0.5511 \end{bmatrix} x \quad (20)$$

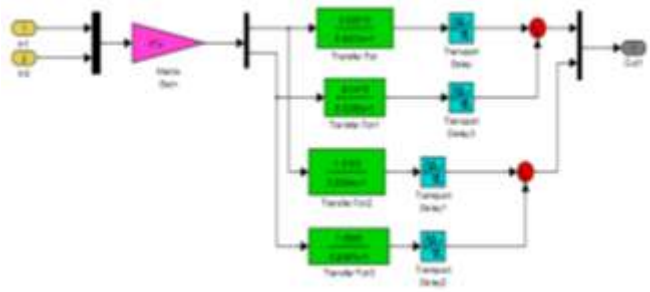

Figure.6 Simulink diagram with delay.

TABLE I. SYSTEM PARAMETERS

Variables	Description	Values
δ	Effective angle of friction	40.5°
ø	Angle of wall friction	18.0°
R	Radius of the rollers	12.5cm
A	Compact surface area	100cm^2
W	Roll width	5cm
τp	Time constant of the roll force response due to the change of hydraulic pressure	6s
$\tau\omega$	Time constant of the roll speed response	6s
τu	Time constant of the feed speed response	6s
ρin	Inlet density	0.3 g/cm^3
C1	Pre-exponential coefficient in the model of material compression	7.5 x 10^{-8}Pa(kg/m^3)$^{4.97}$
K	Compressibility factor	4.97
$2h_o$	roll gap width	3.66 mm
$\rho exist$	Compact density at exit point	0.900 g/cm^3
Pd	Hydraulic pressure (set point)	1 MPa
ωd	Angular velocity of the rolls	5 rpm
ud	Feed speed	3.27 cm/s

CONCLUSION

This paper investigated the modeling and simulation of High Pressure Roller Crusher (HPRC) for the production of silicon carbide grains. The study made a model for simulation of an HPRC. An HPRC is an important part in the production of silicon carbide, where the grains are crushed into powder form and then sieved into specified sizes based on its usage. This paper presented a model based on Johanson's theory for roller compactors, considering all the delays. The non-linearity or delays were handled in Matlab software.

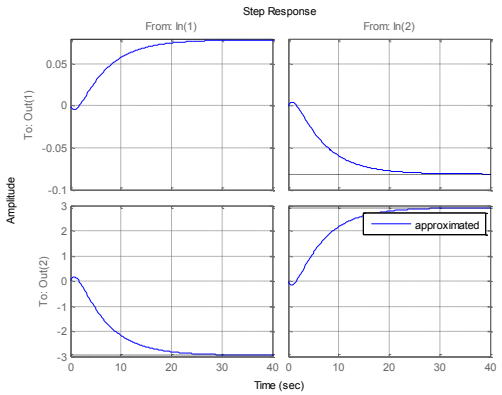

Figure.7 Comparisons of exact and approximate results.

References

[1] Grimble, M.J., Robust Industrial Control: Optimal Design Approach for Polynomial Systems, Prentice Hall, 1994, p. 261 and pp. 443-456

[2] Weir Minerals |KHD Humboldt Wedag 2010

[3] Topalov, A.V., Kaynak, O., 2004. "Neural network modeling and control of cement mills using a variable structure systems theory based on-line learning mechanism", J. Process Control, vol. 14, p. 581.

[4] M.J. Daniel , S. Morrell (2004), 'HPGR model verification and scale-up', Julius Kruttschnitt Mineral Research Centre, The University of Queensland, Isles Road, Indooroopilly, Qld. 4068, Australia

[5] Shuo-Huan Hsu & Gintaras V. Reklaitis & Venkat Venkatasubramanian Modeling and Control of Roller Compaction for Pharmaceutical Manufacturing. Part I: Process Dynamics and Control Framework 18 March 2010.

[6] R. Johnson, (1965) "A rolling theory for granular solids," ASME, Journal of Applied Mechanics 32 : series E. No. 4,

[7] Marshall EA. A theory for the compaction of incompressible granular materials by rolling. J Inst Math Appl. 1973;12(1):21–36

[8] J.R. Johnson, (1965) "A rolling theory for granular solids," ASME, Journal of Applied Mechanics 32 : series E. No. 4,

[9] Jenike A.W, Shield RT. On the plastic flow of Coulomb Solids beyond original failure. Trans ASME: J Appl Mech B. 1959;81:599–602.

[10] JenikeAW, Shield RT. On the plastic flow of Coulomb Solids beyond original failure. Trans ASME: J Apply Mech B. 1959;81:599–602 Apply Mech B. 1965;32(4):842–8.

[11] Marshall EA. A theory for the compaction of incompressible granular materials by rolling. J Inst Math Appl. 1973;12(1):21–36.

[12] Shlieout G, Lammens RF, Kleinebudde P. Dry granulation with a roller compactor. Part I: the functional units and operation modes. Pharma Tech Europe. 2000;12(11):24–3

[13] Panelli R, Ambrozio F. Compaction equation and its use to describe powder consolidation behaviour. Powder Metall. 1998;41 (2):131–3.

[14] Zhang, W.D., and X.M. Xu, "Optimal Solution, Quantitative Performance Estimation, and Robust Tuning of the Simplifying Controller," ISA Trans., Vol. 41, No. 1, pp. 31-36 (2002)

[15] Goodwin, G.C., S.F. Graebe, and M.E. Salgado, Control System Design, Prentice Hall, NJ, U.S.A., pp. 267-268 (2001).

[16] Wang, Q.G., C.C. Hang, and X.P. Yang, "Single-Loop Controller Design via IMC Principles," Automatica, Vol. 37, No. 12, pp. 2041-2048 (2001)

[17] Dingyü Xue,Yang Quan Chen,Derek P. Atherton (2007). "Linear Feedback Control Analysis and Design with MATLAB" Society for Industrial and Applied Mathematics Philadelphia PP. 131,135.